World Journal of Advanced Engineering Technology and Sciences

eISSN: 2582-8266

Cross Ref DOI: 10.30574/wjaets

Journal homepage: https://wjaets.com/

(REVIEW ARTICLE)

Check for updates

Research progress on numerical simulation of vacuum carburization of steel

Xianhao Zheng * and Feng Xiao

School of Mechanical Engineering, Tianjin University of Technology and Education, No. 1310 Dagu South Road, Hexi District, Tianjin 300222, China.

World Journal of Advanced Engineering Technology and Sciences, 2026, 20(02), 045–053

Publication history: Received on 31 July 2026; revised on 05 August 2026; accepted on 06 August 2026

Article DOI: https://doi.org/10.30574/wjaets.2026.20.2.0399

Abstract

Vacuum carburizing is an advanced surface-treatment process used for gears and other high-duty steel components because it provides a uniform case, controllable case depth, and limited oxidation. This review summarizes numerical methods for vacuum carburizing, with emphasis on process parameters, surface carbon transfer, carbon diffusion, carbon-concentration fields, phase transformation, residual stress, and distortion. Early calculations based on Fick's law and empirical diffusivity relations have developed into coupled finite-element models of carburizing and quenching. Recent studies from 2024 to 2026 further introduced carbon-level-dependent diffusion calibration, full-process multiphysics simulation, and machine-learning surrogate models for rapid carbon-field prediction. Across these approaches, predictive accuracy depends primarily on realistic carbon-flux boundary conditions, alloy- and concentration-dependent diffusivity, internally consistent material data, and geometry-resolved experimental validation. Future work should combine physically based models, uncertainty analysis, and reduced-order prediction to support robust process optimization and closed-loop control.

Keywords: Vacuum Carburizing; Numerical Simulation; Carbon Diffusion; Multiphysics Coupling; Residual Stress; Machine Learning

1. Introduction

Vacuum carburizing is an environmentally favorable heat-treatment route for producing a hard, wear-resistant surface while retaining a tough core. Compared with conventional gas carburizing, it can operate at approximately 900-1050 °C, shorten the treatment cycle, reduce harmful emissions, and avoid intergranular oxidation because the process is conducted in an oxygen-free environment [1-3]. These advantages have promoted its use in automotive, aerospace, and machinery components.

The technology emerged in the late 1960s, but early methane- and ethylene-based processes suffered from soot formation and nonuniform cases [4]. The later use of acetylene enabled faster surface reactions and more stable low-pressure pulse carburizing [5]. Modern process design therefore focuses on controlling repeated boost and diffusion stages rather than relying on trial-and-error schedules.

Numerical simulation has become an important part of intelligent heat treatment. Commercial and research codes combine finite-element, finite-volume, or finite-difference methods with descriptions of heat transfer, gas flow, carbon diffusion, phase transformation, stress, and deformation [6]. Figures 1 and 2 summarize representative heat-treatment software and the principal couplings considered in such simulations.

* Corresponding author: Xianhao Zheng.

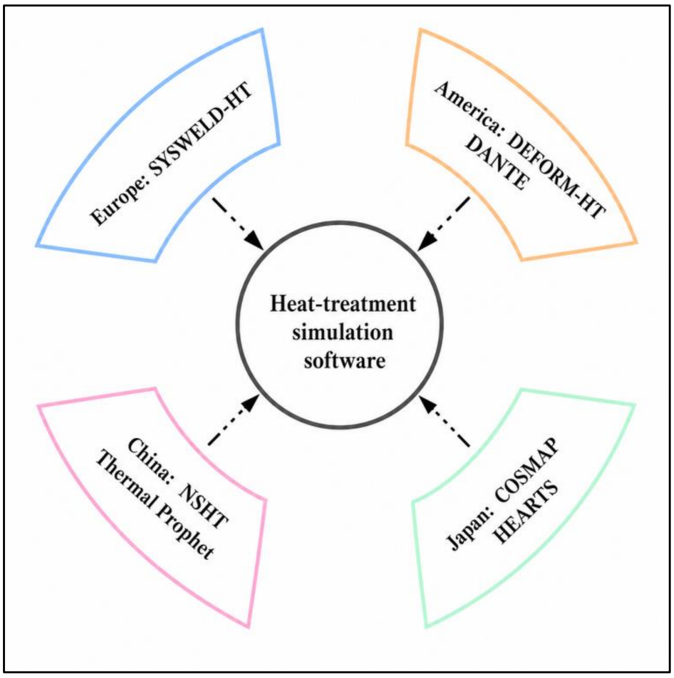

Figure 1 Numerical simulation software for heat treatment. Redrawn by the authors based on Ref. [6].

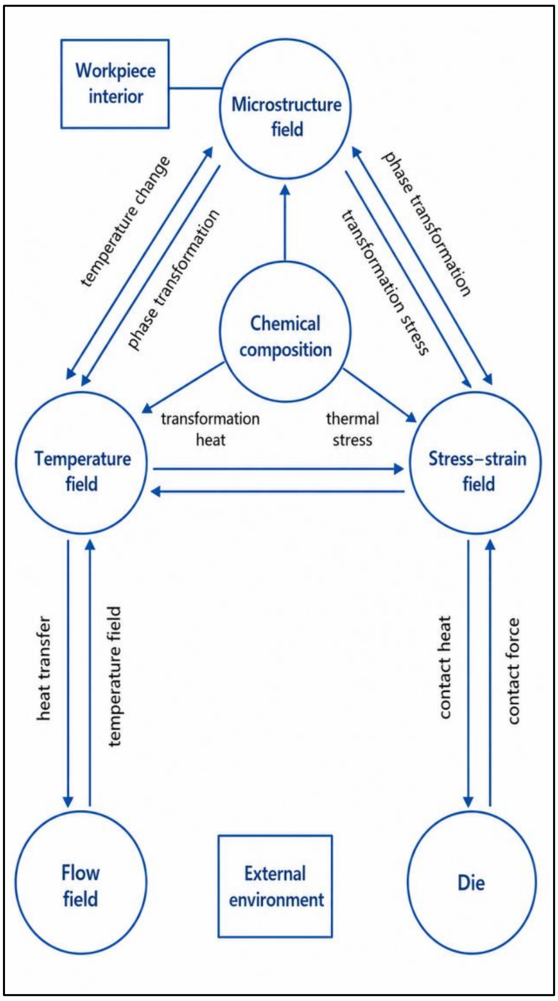

Figure 2 Schematic diagram of multiphysics coupling. Redrawn by the authors based on Ref. [6].

The quality of a vacuum-carburized component depends on temperature, pressure, gas flow, boost and diffusion times, steel composition, and subsequent quenching. Experiments remain essential, but full factorial testing is costly, particularly for large gears and deep cases. Simulation can reduce the number of trials, reveal the evolution of carbon, microstructure, stress, and distortion, and identify practical process windows [7, 8]. This review therefore focuses on the parameters and models that control vacuum carburizing, followed by recent developments in coupled and data-driven prediction.

2. Parameters in numerical simulation of vacuum carburizing

Vacuum-carburizing models require two groups of inputs. Process variables include temperature, pressure, gas flow, boost time, diffusion time, and the target surface carbon content. Material and model parameters include the surface-transfer coefficient, carbon diffusivity in austenite, saturation concentration, thermophysical properties, transformation kinetics, and mechanical properties. The process variables define the cycle, whereas the model parameters determine how carbon and heat are transported and how the component responds during quenching.

The surface-transfer coefficient governs carbon uptake from the atmosphere, while the diffusion coefficient controls redistribution within austenite. Both vary with temperature and may also depend on carbon content, alloy composition, pressure, and surface condition. Reliable simulation therefore requires physically meaningful initial and boundary conditions and parameters calibrated over the intended process range rather than at a single operating point.

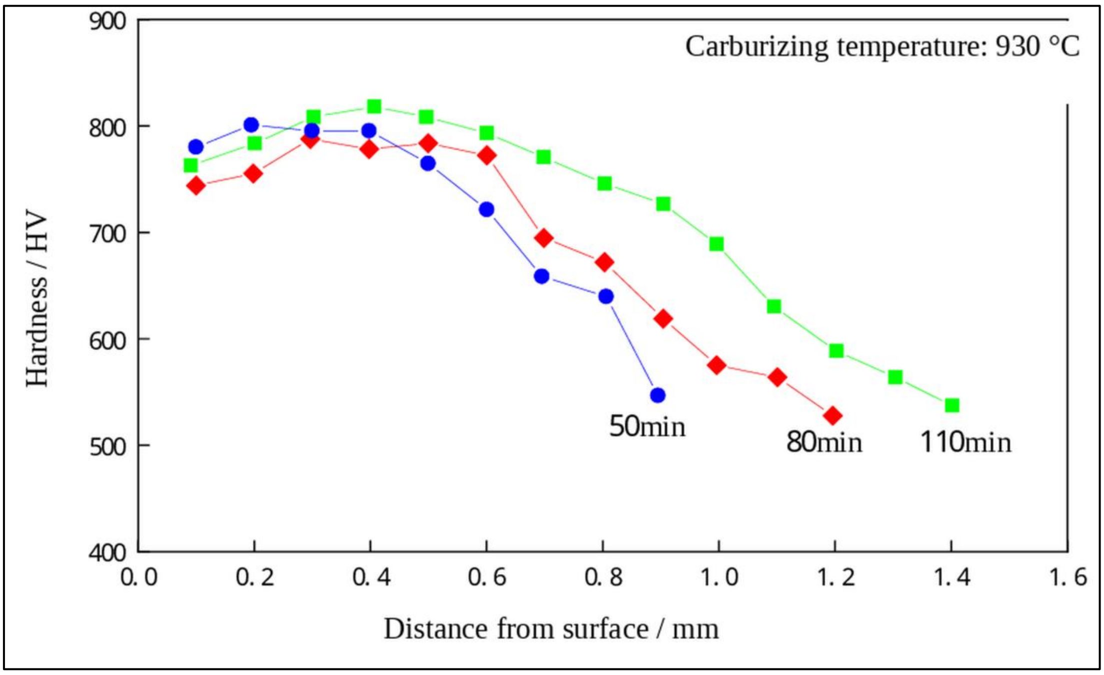

Figure 3 Hardness distribution of carburized layers at different carburizing times. Redrawn by the authors based on Ref. [7].

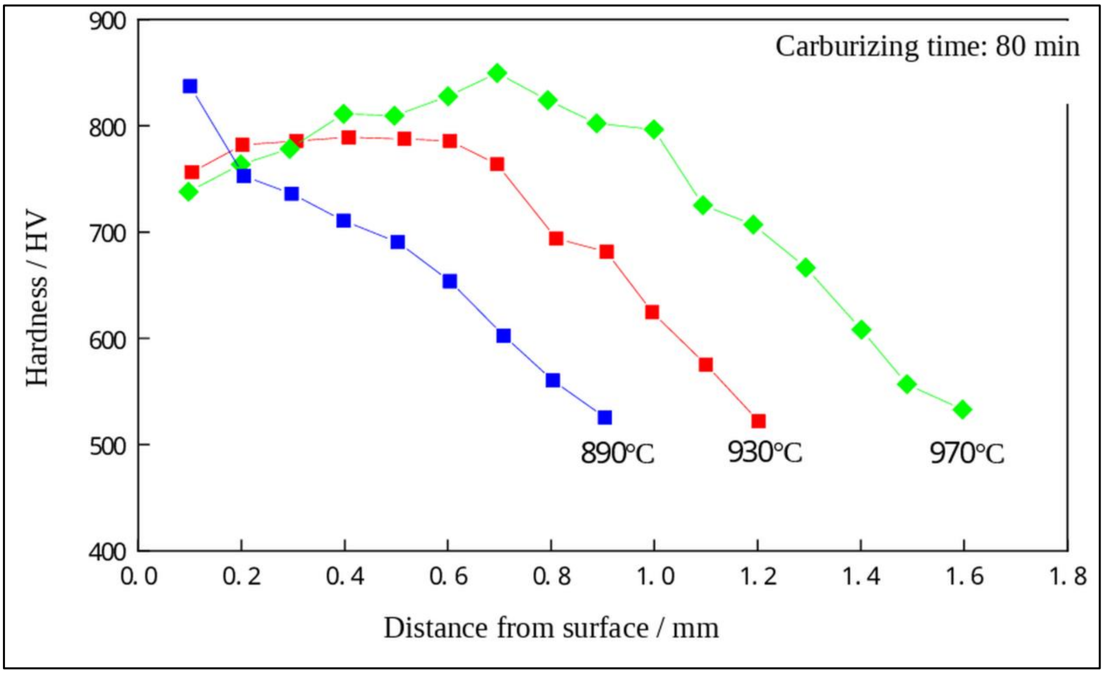

Figure 4 Hardness distribution of carburized layers at different carburizing temperatures. Redrawn by the authors based on Ref. [7].

2.1. Process parameters

Effective cycles balance a short boost stage, which rapidly raises the surface toward carbon saturation, with a longer diffusion stage, which deepens the case and reduces excessive surface carbon. The required durations depend on steel composition, temperature, target case depth, and the permissible surface carbon level [9].

Early process-design methods used enrichment ratios, flow-to-surface-area relations, and diffusion calculations to determine pulse schedules. Subsequent experiments quantified the effects of pressure and temperature on carbon flux, and segmented-flux models improved the description of carbon input during low-pressure carburizing [10, 11]. These studies established the basis for replacing fixed empirical schedules with calculation-assisted cycle design.

Multiphysics models extended this approach by coupling temperature, carbon diffusion, phase transformation, and stress. Guo et al. reproduced measured carbon and hardness profiles in gear steel, while later simulations of 20MnCrS5 components showed that longer diffusion increased case depth and concentration uniformity [12, 13]. The results consistently indicate that temperature has the strongest effect on diffusion rate, whereas the boost-to-diffusion ratio controls the surface gradient.

Recent applications have focused on production steels and complex gears. For 20CrMnTi steel, increasing diffusion time lowered the surface carbon concentration but deepened the case, with close agreement between simulation and experiment [14]. For a 9310 aircraft gear, orthogonal process optimization showed that a moderate temperature increase could shorten the cycle, while the boost-stage carbon input controlled the tooth-surface case thickness [15].

2.2. Key model parameters

The diffusion coefficient and surface-transfer coefficient are the principal parameters governing carburizing kinetics [16]. Vacuum carburizing differs from conventional gas carburizing because acetylene decomposes rapidly on the steel surface and can create a transient carbon-rich layer. The initial driving force is therefore high, but the effective flux changes as the surface approaches saturation and carbides form.

Gas-phase and surface-reaction models have been developed to estimate this flux. CFD studies of propane and acetylene pyrolysis showed that homogeneous reaction models can predict gas composition, while heterogeneous surface models are required for complex components [17, 18]. Under high acetylene flow, the surface may approach saturation rapidly, and the transfer coefficient can be related to molecular arrival, decomposition efficiency, and steel density:

$$\beta(t) = Sm_c l_z(t)/\rho_m \qquad (1)$$

where mc is the molar mass of carbon in acetylene, ρm is the density of steel, and S is the dimensionless reaction efficiency. Boundary-condition studies have shown that the active saturation time and the measured carbon profile can be used to identify the effective transfer parameter [19]. Langmuir-type boundary conditions also provide a useful description of carbon uptake under low pressure [20].

Carbon diffusivity in austenite is not constant. It increases with temperature and is influenced by carbon concentration and alloying additions. Models that neglect these effects can reproduce only a limited range of steels and process conditions [21]. Finite-element calculations using composition- and concentration-dependent diffusivity have therefore replaced simple constant-coefficient treatments in many applications [22, 23].

For multicomponent case-hardening steels, physically based diffusivity relations account for substitutional alloying elements and austenite saturation. Experimental studies confirm that composition can substantially alter both the diffusion coefficient and the final carbon profile [24]. Models must also represent the reduction in carbon flux when a carbide layer develops at the surface.

Recent work has improved parameter identification. A pulse-carburizing model for 15Cr14Co12Mo5Ni2W steel incorporated carbide effects and a segmented enrichment boundary condition [25]. For AISI 9310 steel, inverse calibration of a carbon-level-dependent diffusivity relation reproduced the characteristic inverse-S carbon profile more accurately than conventional equations [26]. These results support the use of steel-specific calibration rather than a single universal diffusivity model.

$$D(T,C,M) = \left\{0.47\exp(-1.6C)\exp\left(-\frac{37000-6600C}{RT}\right)\right\} \times h \qquad (2)$$

Accordingly, carbon-field predictions are most reliable when temperature, carbon concentration, and alloy composition are included explicitly in the diffusion model and the surface flux is calibrated from representative experiments.

3. Research on the carbon-concentration field, residual-stress field, and distortion

3.1. Carbon-concentration field

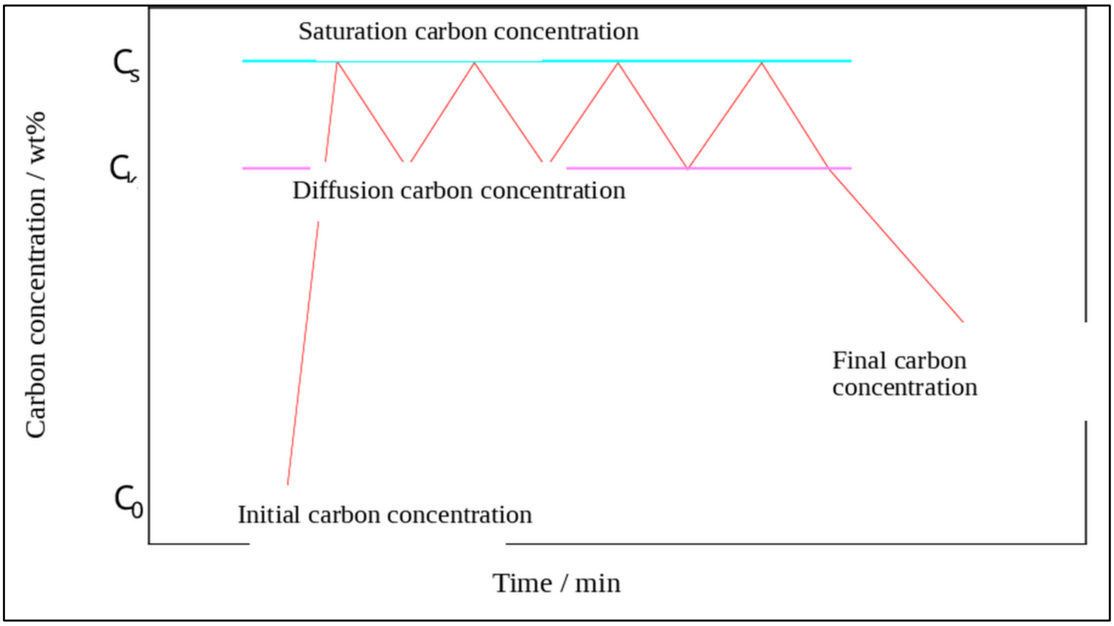

Figure 5 Changes in carbon concentration at the workpiece surface during repeated boost and diffusion stages. Redrawn by the authors based on Ref. [13].

Case depth and surface carbon concentration are the main indicators of carburizing quality. During each boost stage the surface approaches the austenite saturation concentration; during diffusion the surface concentration falls while carbon penetrates farther into the steel. Repeating these stages produces the sawtooth surface history illustrated in Figure 5 and gradually increases the effective case depth. Fick's second law is normally solved with finite-element or finite-difference methods using measured or calibrated boundary conditions.

Finite-element models that include acetylene-specific boundary conditions and alloy effects have reproduced measured profiles in SCM415 steel [27]. CarbTool and related programs extended the same framework to different alloys and both atmosphere and low-pressure carburizing routes [28]. These studies demonstrate that the same diffusion equation can be used widely if the surface condition and material parameters are selected consistently.

Production-oriented simulations have been used to determine pulse ratios, case depth, and edge effects. For 20CrNi2Mo steel, a boost-to-diffusion time ratio near 1:10 produced reasonable agreement between calculated and measured case depth [29]. Simulations of vacuum-carburized Fe-based materials also reproduced the inward decrease in carbon concentration shown in Figure 6 [30].

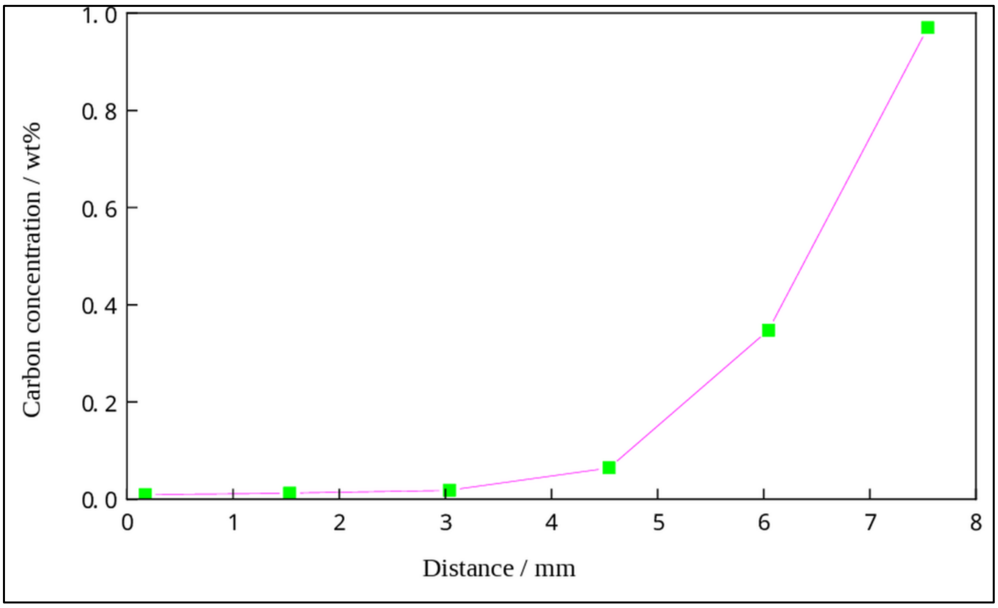

Figure 6 Cross-sectional carbon-concentration curve. Redrawn by the authors based on Ref. [30].

More recent models combine diffusion with phase transformation and quenching. Simulations of carburized C-rings and gears linked the carbon gradient to martensite formation, hardness, retained austenite, and local distortion [31]. Numerical solutions based on calibrated gradient models have also agreed closely with layer-removal measurements [32]. The remaining errors are concentrated near corners, tooth roots, and other regions where gas access, heat transfer, and mesh resolution differ from one-dimensional assumptions.

3.2. Residual-stress field and distortion

Residual stress and distortion result from the interaction of thermal gradients, carbon-dependent phase transformation, transformation strain, and mechanical constraint. Their prediction is important because compressive surface stress can improve fatigue resistance, whereas excessive tensile stress or distortion can cause cracking and dimensional loss. Carburizing and quenching should therefore be simulated as a continuous process chain rather than as independent steps.

Validated finite-element studies have predicted microstructure, residual stress, distortion, and subsequent loading response in vacuum-carburized coupons and gears [33]. Comparative calculations for plain-carbon and alloy steels showed that carbon gradients, martensite, and retained austenite strongly affect the magnitude and location of residual stress [34]. Gear simulations have also reproduced hardness, case depth, and dimensional change with useful engineering accuracy [35].

4. Recent developments, challenges, and future directions

Recent research has concentrated on faster carbon-field prediction, improved coupling between carburizing and quenching, and validation on industrial geometries. These developments complement rather than replace physically based diffusion models.

4.1. Recent developments from 2024 to 2026

Data-driven surrogate models can reduce computational cost. A BP neural network trained on finite-element data predicted one- and two-dimensional carbon fields with sub-percent average relative error and reduced the time for a two-dimensional calculation to approximately 0.12 s [36]. A later model expanded the training set to multiple geometries and confirmed that the largest errors occur near corners and sparsely sampled regions [37]. Such models are promising for optimization, provided that their training data represent the intended steel, geometry, and boundary conditions.

The carburized carbon gradient also changes the phase-transformation sequence during quenching and therefore the residual-stress field [38]. Full-process models now predict carbon content, retained austenite, hardness, residual stress, deformation, and case depth within one computational framework [39, 40]. This integration is essential for assessing whether a cycle that produces the required carbon profile will also meet dimensional and performance requirements.

Industrial studies provide practical validation. Experiments on automotive gear steels showed that higher vacuum-carburizing temperatures increase case depth but may promote abnormal grain growth, while moderate cycle-time reductions can preserve surface hardness and microstructural uniformity with a controlled decrease in case depth [41, 42]. Differences between tooth flanks and roots further demonstrate the need for geometry-resolved validation.

4.2. Challenges and future priorities

Despite these advances, transfer of calibrated models between steel grades, furnaces, and component geometries remains difficult. Four priorities are particularly important:

- Develop coupled process-chain models linking carburizing, quenching, cryogenic treatment, and tempering, with reduced-order versions for routine process design.
- Establish standardized material databases containing composition- and carbon-dependent thermophysical, transformation, diffusion, and mechanical properties with uncertainty ranges.
- Calibrate carbon flux, transfer coefficients, and heat-transfer boundary conditions over multiple temperatures, pressures, pulse schedules, and steel grades.
- Validate physically constrained surrogate models on complex industrial components using carbon profiles, microstructure, hardness, residual stress, and distortion.

5. Conclusion

Numerical simulation of vacuum carburizing has progressed from one-dimensional diffusion calculations to coupled descriptions of surface transfer, carbon diffusion, phase transformation, residual stress, distortion, hardness, and case performance. Recent advances include steel-specific diffusivity calibration, full-process carburizing-quenching models, and machine-learning surrogates trained on finite-element data. Their practical reliability still depends on realistic boundary conditions, alloy- and concentration-dependent material parameters, uncertainty assessment, and experiments representative of the intended component geometry and process window. Combining validated multiphysics models with rapid reduced-order prediction offers a practical route to robust cycle optimization and closed-loop control.

Compliance with ethical standards

Disclosure of conflict of interest

The authors declare that they have no conflict of interest.

References

[1] Zhao Z. (2012). Application and prospects of low-pressure vacuum carburizing. Metal Working (Hot Working), (3), 6-9. (in Chinese).

[2] Liu Y, Feng Y, Zhao W, et al. (2009). Energy conservation, emission reduction, and environmental technologies in heat treatment. Heat Treatment of Metals, 34(3), 103-107.

[3] Kochmański P, Chylińska R, Figiel P, et al. (2024). Influence of chemical composition on structure and mechanical properties of vacuum-carburized low-alloy steels. Materials, 17(2), 515.

[4] Zhang J, Cong P. (2003). Status and development of vacuum-carburizing technology in China and abroad. Heat Treatment of Metals, (10), 52-55.

[5] Zajusz M, Tkacz-Śmiech K, Danielewski M. (2014). Modeling of vacuum pulse carburizing of steel. Surface and Coatings Technology, 258, 646-651.

[6] Gu J, Pan J. (2013). Intelligent heat treatment and its development prospects. Heat Treatment of Metals, 38(2), 1-9.

[7] Ren W, Zhang T, Wu G, et al. (2015). Microstructure and properties of vacuum low-pressure-carburized 20CrMnTi steel. Hot Working Technology, 44(16), 187-190.

[8] Atraszkiewicz RP, Dybowski K. (2023). Minimizing deformations in high-temperature vacuum carburizing. Materials, 16(24), 7630.

[9] Li ZC, Ferguson BL, Yu T, et al. (2018). Low-pressure carburizing cycle determination for high-alloy steels. In: Thermal Processing in Motion, Spartanburg, SC, USA, 5-7.

[10] Tian Y, Wang H, An X, et al. (2019). Experimental study on carbon flux in vacuum carburizing. Materials Research Express, 6(9), 096516.

[11] Wang H, Liu J, Tian Y, et al. (2020). Mathematical modeling of carbon-flux parameters for low-pressure vacuum carburizing of medium-high-alloy steel. Coatings, 10(11), 1075.

[12] Guo J, Deng X, Wang H, et al. (2021). Modeling and simulation of vacuum low-pressure carburizing of gear steel. Coatings, 11(8), 1003.

[13] Zhang Z, Deng X, Fan Y, et al. (2023). Multiphysics simulation of vacuum low-pressure carburizing and gas quenching of 20MnCrS5 steel. Surface Technology, 1-13.

[14] Deng X, Song W, Fan Y, et al. (2024). Numerical simulation of low-pressure vacuum carburizing of 20CrMnTi steel. Heat Treatment of Metals, 49(8), 220-224.

[15] Zhang Z, Zhang Y, Hu Y, et al. (2024). Numerical simulation and process-parameter optimization of vacuum-carburizing surface strengthening for a 9310 aircraft gear. Journal of Chongqing University of Technology (Natural Science), 38(7), 194-203.

[16] Ma W, Sheng J, Wang Y, et al. (2022). Measurements of carbon diffusivity and surface-transfer coefficient by electrical-conductivity relaxation during carburization: experimental design by theoretical analysis. Coatings, 12(12), 1886.

[17] Khan RU. (2008). Vacuum gas carburizing: fate of hydrocarbons. Dissertation, Universität Karlsruhe, Karlsruhe, Germany.

[18] Buchholz D, Khan RU, Bajohr S, et al. (2010). Computational-fluid-dynamics modeling of acetylene pyrolysis for vacuum carburizing of steel. Industrial & Engineering Chemistry Research, 49(3), 1130-1137.

[19] Smirnov AE, Ryzhova MY, Semenov MY. (2017). Choice of boundary condition for solving the diffusion problem in simulation of vacuum carburizing. Metal Science and Heat Treatment, 59, 237-242.

[20] Semenov MY, Smirnov AE, Ryzhova MY. (2021). Problems of simulation of carbon mass transfer from a low-pressure saturating atmosphere into steel. Metal Science and Heat Treatment, 63(1-2), 101-105.

[21] Ochsner A, Gegner J, Mishuris G. (2004). Effect of diffusivity as a function of the method of computation of carbon-concentration profiles in steel. Metal Science and Heat Treatment, 46(3), 148-151.

[22] Kim DW, Cho YG, Cho HH, et al. (2011). A numerical model for vacuum carburization of an automotive gear ring. Metals and Materials International, 17, 885-890.

[23] Yada K, Watanabe O. (2013). Reactive-flow simulation of vacuum carburizing with acetylene gas. Computers & Fluids, 79, 65-76.

[24] Gegner J, Vasilyev AA, Wilbrandt PJ, et al. (2012). Alloy dependence of the diffusion coefficient of carbon in austenite and analysis of carburization profiles in case-hardening steels. In: MMT Conference, 1-261.

[25] He Y, Zeng XJ, Li LQ, et al. (2024). Phase composition and numerical model of a low-pressure pulse-carburized layer in 15Cr14Co12Mo5Ni2W steel. Surface and Coatings Technology, 130868.

[26] Xu D, Kim J, Frame LD, Tang J. (2025). Advancing vacuum carburizing simulation: Calibration and implementation of a carbon-level-dependent diffusion model for AISI 9310 steel. Journal of Engineering Materials and Technology, 147(4), 041001. doi: 10.1115/1.4068282.

[27] Jung M, Oh S, Lee YK. (2009). Predictive model for the carbon-concentration profile of steels vacuum carburized with acetylene. Metals and Materials International, 15, 971-975.

[28] Wei Y, Zhang L, Sisson RD. (2013). Modeling of carbon-concentration-profile development during atmosphere and low-pressure carburizing. Journal of Materials Engineering and Performance, 22, 1886-1891.

[29] Wang Z, Shi J, Mei J, et al. (2017). Vacuum carburizing and numerical simulation of 20CrNi2Mo steel. Heat Treatment of Metals, 42(11), 117-122.

[30] Song K. (2020). Microstructural evolution and numerical simulation of vacuum-carburized Fe-based materials. Dissertation, Guizhou University, Guiyang, China.

[31] Yuan L, He D, He X, et al. (2022). Finite-element simulation of vacuum low-pressure carburizing and quenching of a 16Cr3NiWMoVNbE steel C-ring. Heat Treatment of Metals, 47(9), 257-263.

[32] He Y, Fu Z, Zhang X, et al. (2023). Numerical simulation of the carbon-concentration gradient in vacuum-carburized G13Cr4Mo4Ni4V steel and development of application software. Hot Working Technology, 1-5.

[33] Freborg A, Ferguson B, Li Z. (2014). Modeling heat treatment to characterize distortion, residual stress, loading response, and fracture in a vacuum-carburized and gas-quenched steel coupon. In: Proceedings of the 5th International Conference on Thermal Process Modeling and Computer Simulation, Orlando, FL, USA.

[34] Hiremath P, Sharma S, Gowrishankar MC, et al. (2020). Effect of post-carburizing treatments on residual-stress distribution in plain-carbon and alloy steels: a numerical analysis. Journal of Materials Research and Technology, 9(4), 8439-8450.

[35] Li C. (2022). Numerical simulation and process optimization of heat treatment for a 9310 steel aircraft thin-web gear. Dissertation, Central South University, Changsha, China.

[36] Zhang Y, Tang Z, He L, Mahdipanah MH, Wang Y. (2024). Real-time prediction method of carbon concentration in carburized steel based on a BP neural network. Heat Treatment and Surface Engineering, 6(1), 2350184. doi: 10.1080/25787616.2024.2350184.

[37] Zhang Y, Tang Z, Yin Q, Wang Y, Nie Z. (2025). Machine learning based prediction of carbon concentration in carburized steel. Scientific Reports, 15, 33678. doi: 10.1038/s41598-025-18531-8.

[38] Liu H, Tang J, Liu C, Liu Y, Jiang W, Sun B. (2024). Understanding the distinction between quenching and carburizing quenching stress field: Evolution mechanism of quenching stress field influenced by carbon content in low-carbon alloy steel. Surface and Coatings Technology, 489, 131112. doi: 10.1016/j.surfcoat.2024.131112.

[39] Jia Z, Chen Y, Luo L, Zhao H. (2025). Multi-scale full-process prediction and performance analysis of carburizing and quenching heat treatment. JOM, 77, 8137-8154. doi: 10.1007/s11837-025-07761-w.

[40] Ben Ayed S, Charles Y, Daniel L. (2025). Finite element modeling of the carburizing-quenching process in steels. Journal of Materials Research and Technology, 39, 3103-3114. doi: 10.1016/j.jmrt.2025.10.031.

[41] Viliš J, Dobrocký D, Joska Z, Procházka J, Klimeš M. (2025). The effect of changing the temperature of the vacuum carburizing process on the layer properties of steels used in the automotive industry. The International Journal of Advanced Manufacturing Technology, 137(5-6), 2823-2833. doi: 10.1007/s00170-025-15319-y.

[42] Klimeš M, Viliš J, Dobrocký D, Procházka J. (2026). Process robustness in reduced-time vacuum carburizing of automotive gear steels. The International Journal of Advanced Manufacturing Technology, 144, 5597-5609. doi: 10.1007/s00170-026-18226-y